Supplementary Figures

Table 1: Minimum, maximum, and mean size (in mg) of all predators in this study.

Species size statistics			
Species	Min Size (mg)	Max Size (mg)	Mean Size (mg)
Oonopidae	0.2	0.5	0.4
Neoscona theisi	0.5	24.2	9.4
Geophilomorpha	2.6	28.4	11.3
Scytodes longipes	1.1	40.7	13.2
Euborellia annulipes	0.4	53.4	15.4
Smeringopus pallidus	8.5	28.2	16.2
Phisis holdhausi	4.1	78.5	33.1
Pantala flavescens	151.1	259.8	205.7
Heteropoda venatoria	1.3	929.0	280.8

Table 2: Samples by species on each sequencing run

Species and sample sizes by sequencing run		
Species	Sample Size	Run
Heteropoda venatoria	39	a
Neoscona theisi	24	a
Scytodes longipes	7	a
Geophilomorpha	12	b
Phisis holdhausi	42	b
Smeringopus pallidus	13	b
Euborellia annulipes	18	c
Oonopidae	4	c
Pantala flavescens	9	c
Heteropoda venatoria	14	d

Table 3: Predator species, traits, and sample sizes

Number of predator individuals and interactions per species and traits

species	hunting_mode	venom	webs	individuals	interactions
Geophilomorpha sp	active	yes	no	12	14
E. annulipes	active	no	no	18	23
H. venatoria	active	yes	yes	53	93
Oonopidae sp	active	yes	yes	4	7
N. theisi	not_active	yes	yes	24	68
P. flavescens	active	no	no	9	14
P. holdhausi	active	no	no	42	71
S. longipes	not_active	yes	yes	7	17
S. pallidus	not_active	yes	yes	13	28

Table 4: The class, order, and family-level taxonomic identity of prey items detected in DNA data.

Class	Order	Family
Arachnida	Araneae	Araneidae
Arachnida	Araneae	Oxyopidae
Arachnida	Araneae	Pholcidae
Arachnida	Araneae	Salticidae
Arachnida	Araneae	Theridiidae
Arachnida	Sarcoptiformes	Acaridae
Arachnida	Sarcoptiformes	Pyroglyphidae
Arachnida	Sarcoptiformes	Suidasiidae
Chilopoda	Geophilomorpha	Mecistocephalidae
Collembola	Entomobryomorpha	Entomobryidae
Collembola	Entomobryomorpha	Isotomidae
Collembola	Symphypleona	Bourletiellidae
Collembola	Symphypleona	Sminthuridae
Insecta	Blattodea	Blaberidae
Insecta	Blattodea	Blattidae
Insecta	Blattodea	Ectobiidae
Insecta	Coleoptera	Coccinellidae
Insecta	Coleoptera	Curculionidae
Insecta	Coleoptera	Elateridae
Insecta	Coleoptera	Hydrophilidae
Insecta	Coleoptera	Staphylinidae
Insecta	Dermaptera	Anisolabididae
Insecta	Diptera	Agromyzidae
Insecta	Diptera	Calliphoridae
Insecta	Diptera	Cecidomyiidae
Insecta	Diptera	Ceratopogonidae
Insecta	Diptera	Chloropidae
Insecta	Diptera	Culicidae
Insecta	Diptera	Dolichopodidae
Insecta	Diptera	Limoniidae
Insecta	Diptera	Lonchaeidae
Insecta	Diptera	Phoridae
Insecta	Diptera	Platystomatidae
Insecta	Diptera	Psychodidae
Insecta	Diptera	Sciaridae

Insecta	Diptera	Stratiomyidae
Insecta	Hemiptera	Aleyrodidae
Insecta	Hemiptera	Coccidae
Insecta	Hemiptera	Pseudococcidae
Insecta	Hymenoptera	Eulophidae
Insecta	Hymenoptera	Evaniidae
Insecta	Hymenoptera	Formicidae
Insecta	Lepidoptera	Agonoxenidae
Insecta	Lepidoptera	Crambidae
Insecta	Lepidoptera	Erebidae
Insecta	Lepidoptera	Tineidae
Insecta	Odonata	Libellulidae
Insecta	Orthoptera	Acrididae
Insecta	Orthoptera	Mogoplistidae
Insecta	Orthoptera	Tettigoniidae
Insecta	Psocoptera	Ectopsocidae
Insecta	Psocoptera	Lepidopsocidae
Insecta	Psocoptera	Liposcelididae
Insecta	Psocoptera	Myopsocidae
Insecta	Thysanoptera	Thripidae
Malacostraca	Isopoda	Philosciidae

Table 5: Model summary examining whether samples comprising multiple individuals had more interactions than samples with only one individual. The null model (no effect of number of individuals) was the best model based on AICc values.

Model selection of number of individuals per sample model

No..Individuals	df	logLik	AICc	delta	weight
NA	3	−268.21	542.55	0.00	0.6356673
0.02	4	−267.72	543.66	1.11	0.3643327

Table 6: ASVs assigned to positive control samples and their rarefied read abundances

ASV	sample	reads
ASV_7	CL42a	243272
ASV_7	CL42b	188148
ASV_7	CL42c	151021
ASV_7	CL42d	233022
ASV_10	CL12a	158262
ASV_10	CL12b	179340
ASV_10	CL12c	100329
ASV_10	CL12d	1812
ASV_11	QC1a	112242
ASV_11	QC1b	201979
ASV_11	QC1c	122805
ASV_11	QC1d	1657

Table 7: Model output for linear model selection of prey size predicted by predator size and species. The best model based on AICc values included size and species, but not their interaction.

Model selection of predator-prey size linear model

log10 Predator mass	Predator species	log10 Predator mass*Predator species	df	logLik	AICc	delta
0.34	+	NA	12	−423.67	872.30	0.00
−0.46	+	+	20	−417.34	877.36	5.06
NA	+	NA	11	−430.34	883.50	11.20
0.21	NA	NA	4	−469.55	947.23	74.93
NA	NA	NA	3	−473.80	953.66	81.36

Table 8: Model selection of trait use models demonstrating that the model that included web use was the best model based on AICc values.

Model selection of predator trait models			
model	df	AICc	delta
m_webs	5.00	939.17	−0.00
m_null	4.00	940.19	1.03
m_hunting_mode	5.00	941.02	1.85
m_venom	5.00	941.64	2.47

Figure 1: Sequencing depth of initial four samples rarefaction

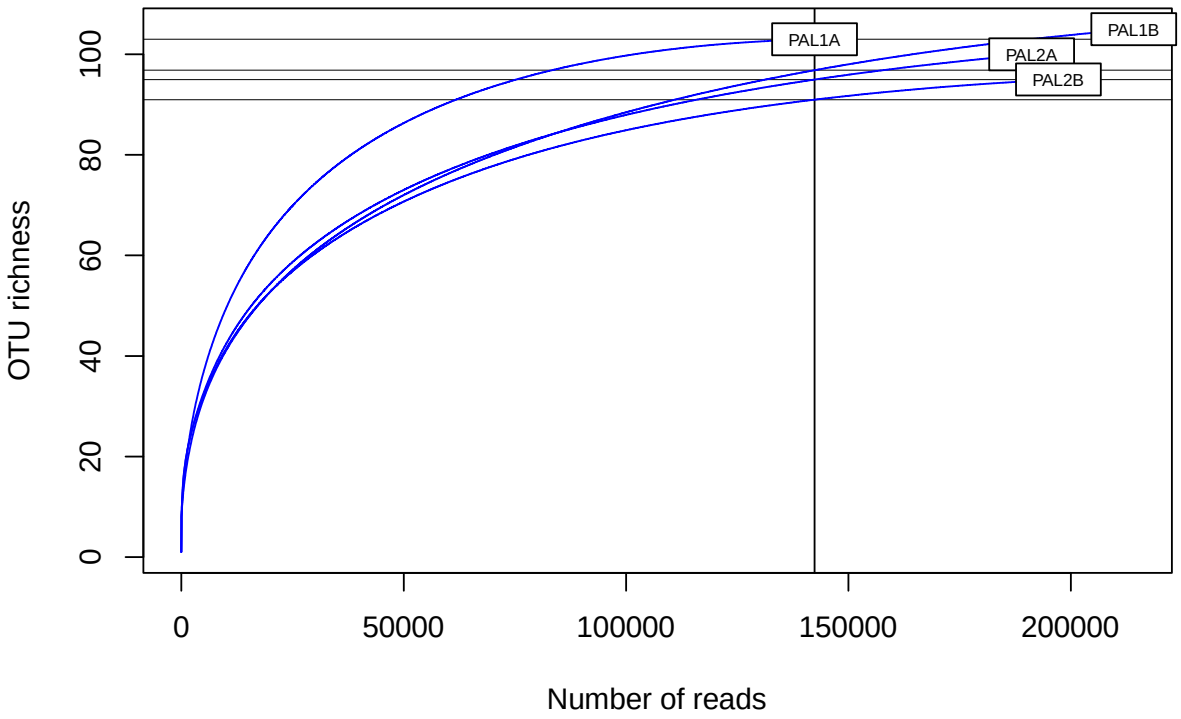

We initially determined how many samples to run per sequencing run to achieve adequate sequencing depth to detect prey DNA based on a MiSeq Nano run with four samples. From this, we determined that samples needed to be sequenced to a depth of roughly 140,000 reads to capture full OTU diversity (the vertical line). Thus, we based the number of samples per run (roughly 100 samples per run) on this optimal sequencing depth per sample.

Figure 2: Run-to-run variation in ASV number and diet family number

Quantifying cross-run variation

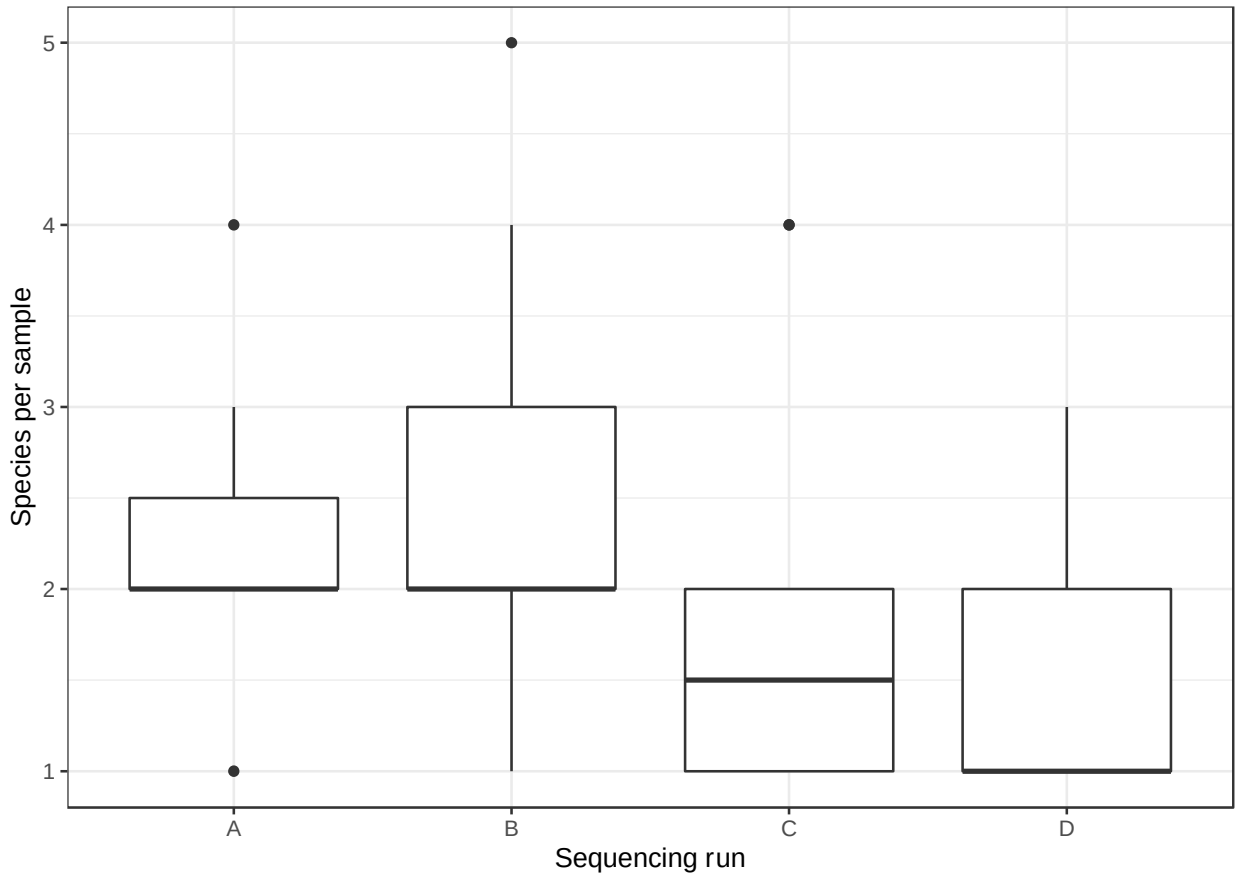

There was significant cross-run variation in the number of prey families assigned per sample for the 19 samples we re-ran across all runs. There were significant post-hoc differences (pair-wise differences between runs with p-value ≤ 0.05) between run 1-4, 2-3, and 2-4. On average, samples had: A: 2.26 ± 0.15, B: 2.33 ± 0.24, C: 1.72 ± 0.23, and D: 1.44 ± 0.15 prey families in each sample. Because each predator species was run on a sequencing run with all other individuals from that predator species and because we did not compare species richness as a response variable across predator species in this study, we report this as the variation across sequencing runs but do not correct for it in future analyses.

Figure 3: Dada2 vs UNOISE3 – histogram

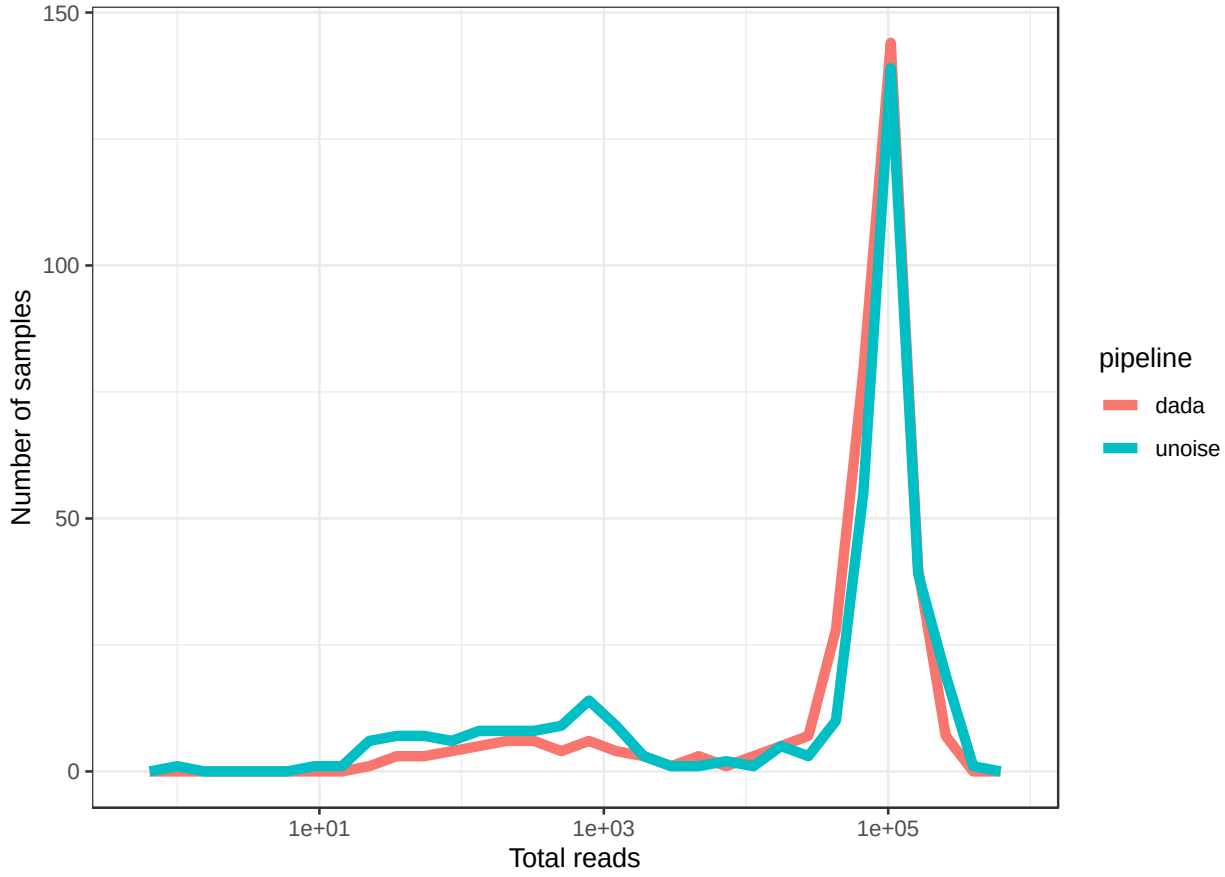

We compared the reads assigned using both the DADA2 and UNOISE3 algorithms. DADA2 produced more samples with high read abundances than UNOISE3 (slightly higher peak of the number of samples with high read abundances) and so we used this denoising algorithm for this study.

Figure 4: DADA2 – cross-run errors

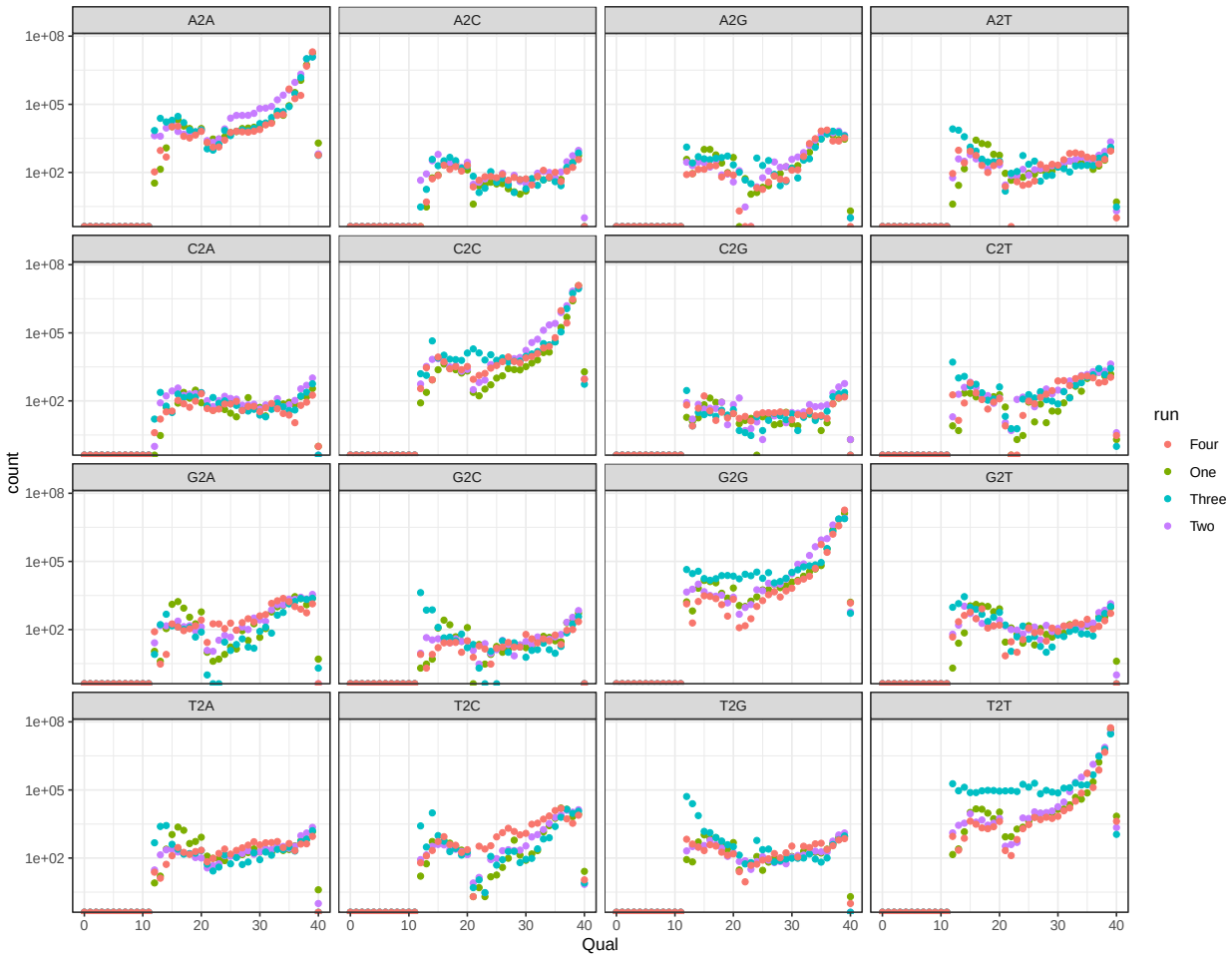

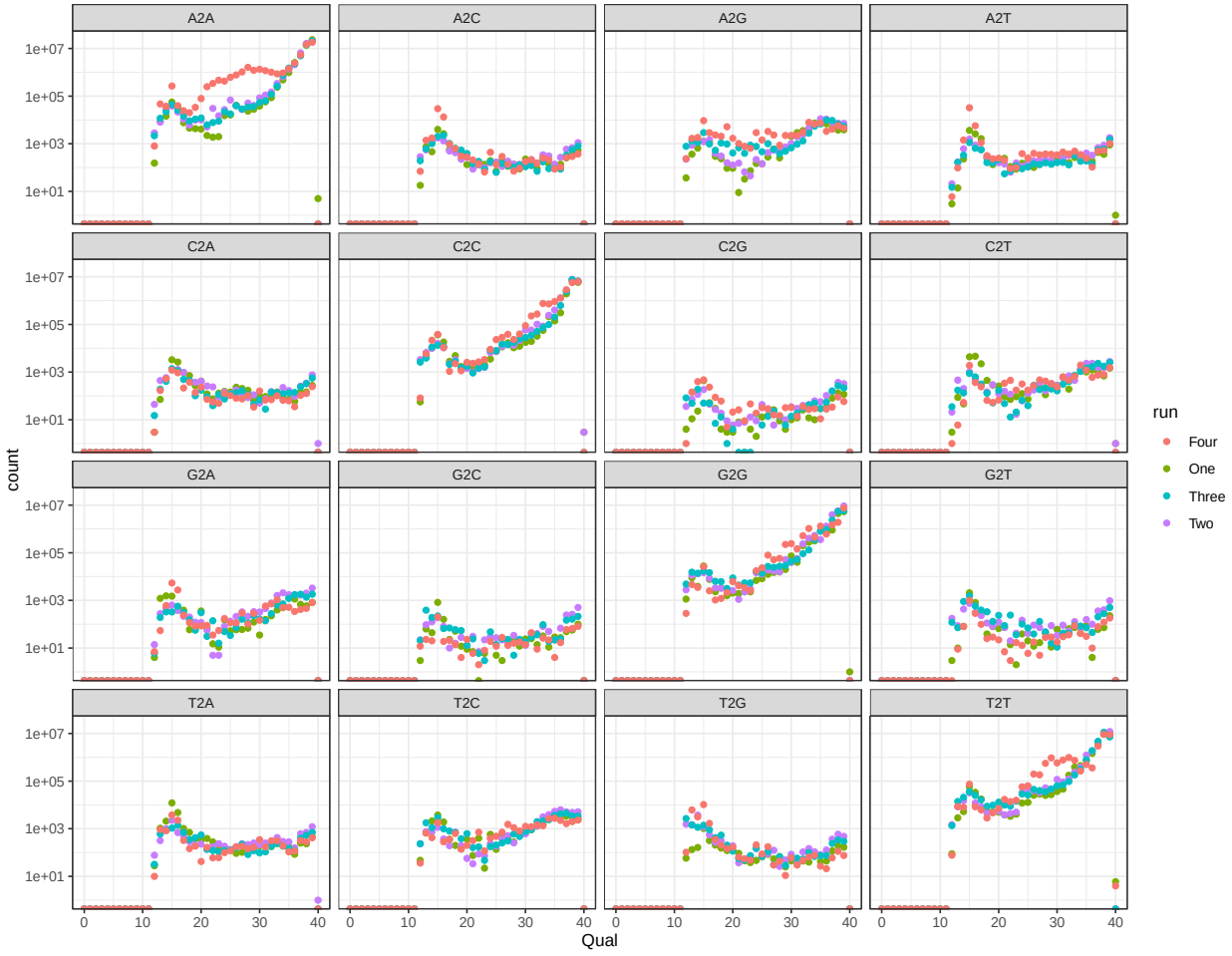

Error rates for each of the sequencing runs. Based on recommendations from the developers of DADA2, we ran the DADA2 algorithm on all samples from all runs combined after verifying that the error rates were similar across runs before doing so.

Figure 5: Sequencing depth across samples

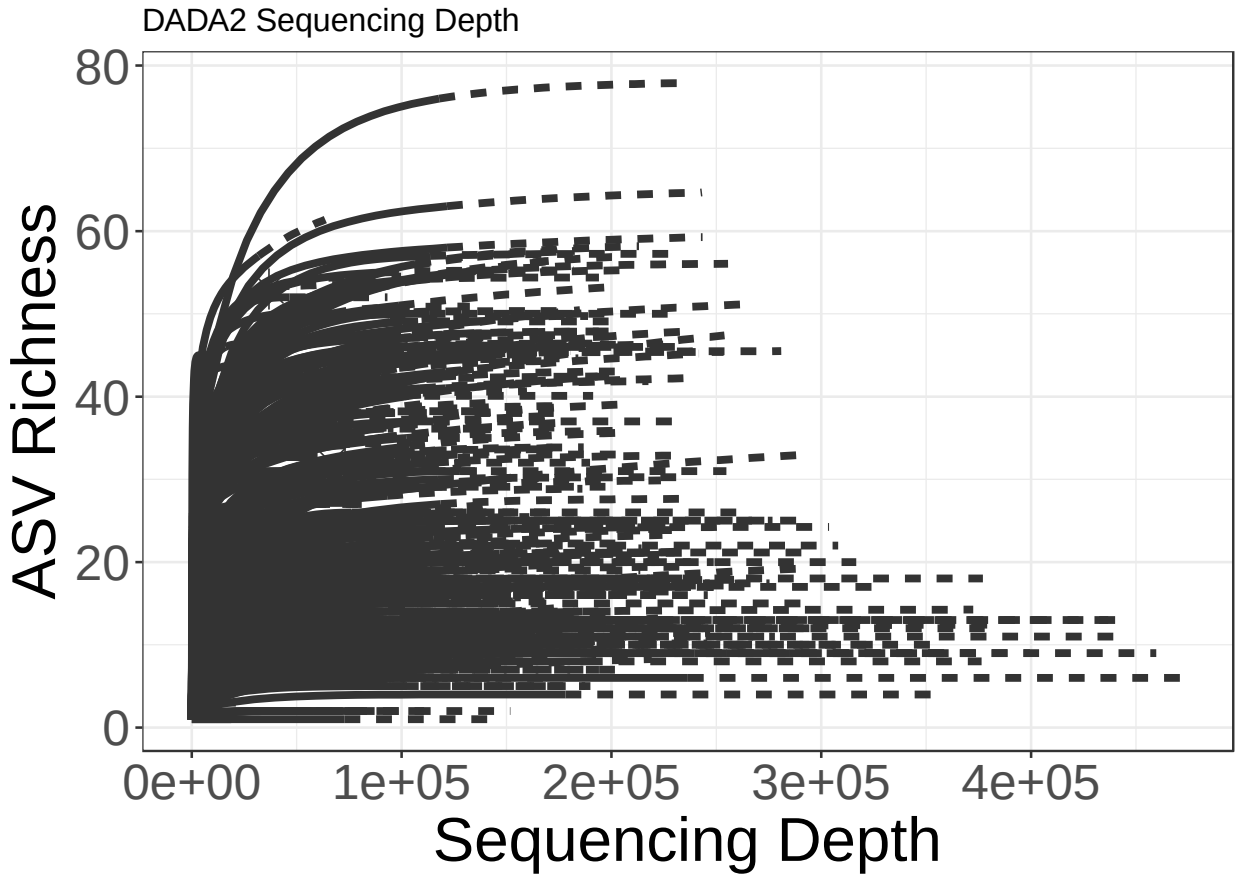

Sequencing depths across all samples in our study, demonstrating the wide range in depths (10,000 – 100,000 for the current study) that can occur in DNA sequencing studies.

Figure 6: Inflection point of quantiles of sequencing depth graph

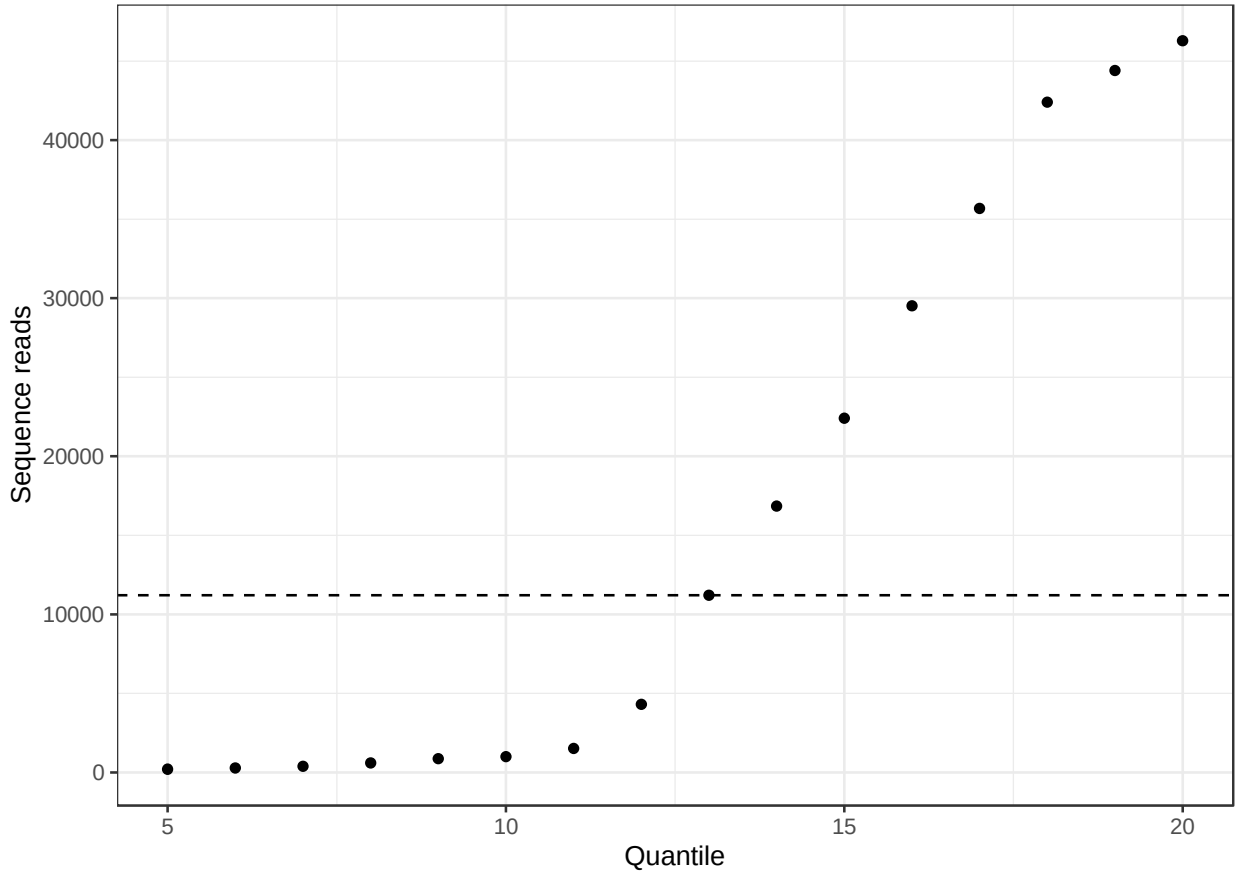

We chose to remove samples from analyses that had been sequenced below a certain threshold. We determined the quantiles at 0.01 increments within the dataset and found the inflection point where a 0.01 increase in the quantile led to the greatest increase in read abundance. We determined that any samples below this sequencing depth were likely sequenced at too low a level to be comparable to the other samples in our study. Through this process, this was determined to be the 0.13 quantile and a sequencing depth below 11,211. All samples with sequencing depths below this threshold were removed from further analyses.

Figure 7: Histogram of the number of individuals per sample

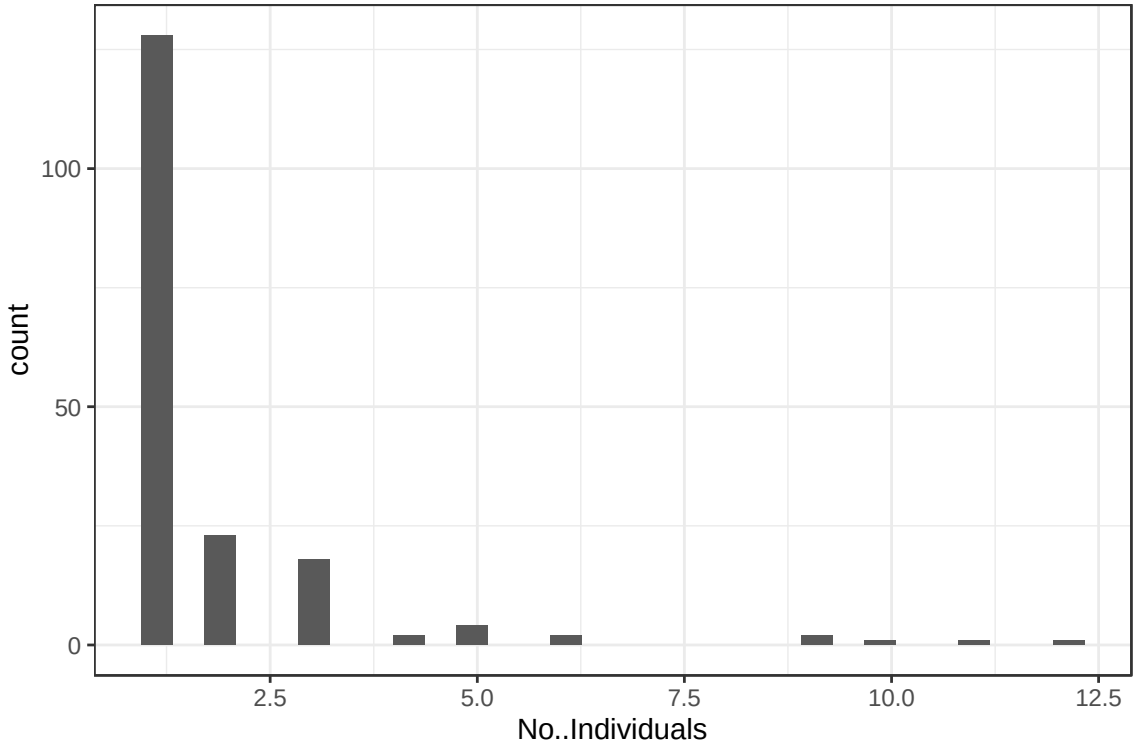

Figure 7: A distribution of the number of individuals in each sample in this study. Individuals were combined for some samples to obtain ample DNA product for DNA cleaning and PCR protocols. We only combined individuals from shared species, size (± 0.5 mm), and sampling sessions. Seventy percent (n = 128/181) samples came from individual predators, and the remaining samples comprised one or more individuals with a maximum of 12.

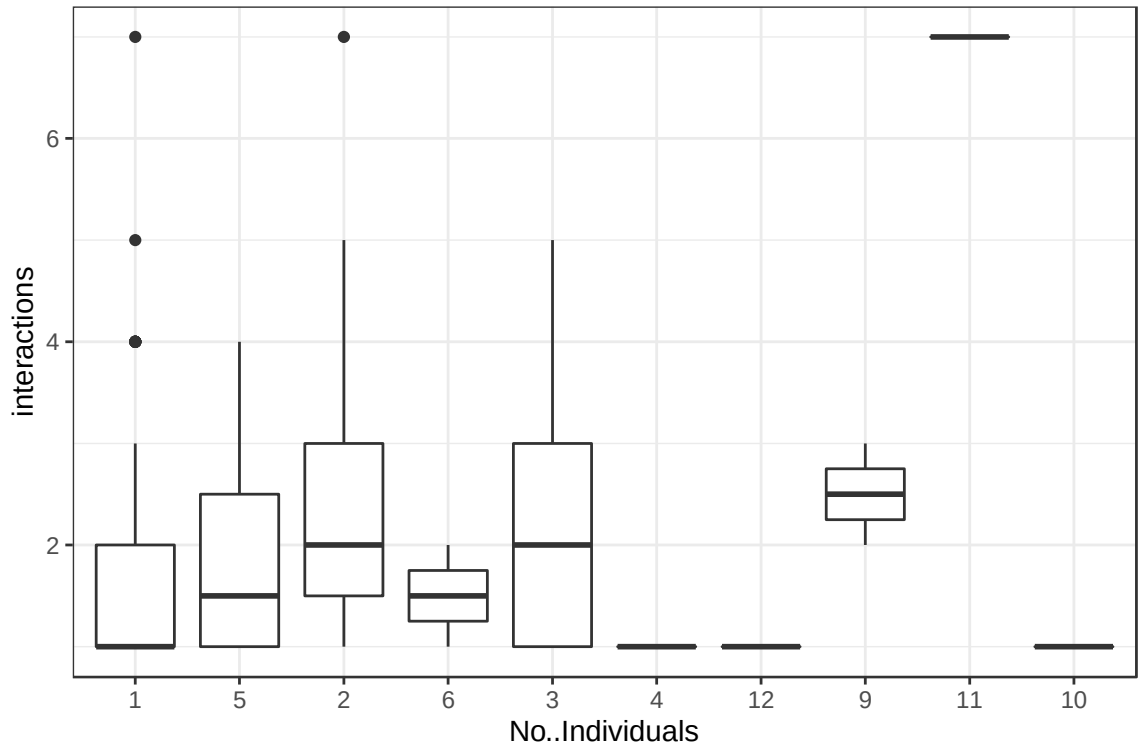

Figure 8: The number of interactions per number of individuals in a sample. The number of individuals in a sample did not influence over all interactions per sample.

Figure 9: ASVs for positive and negative controls.

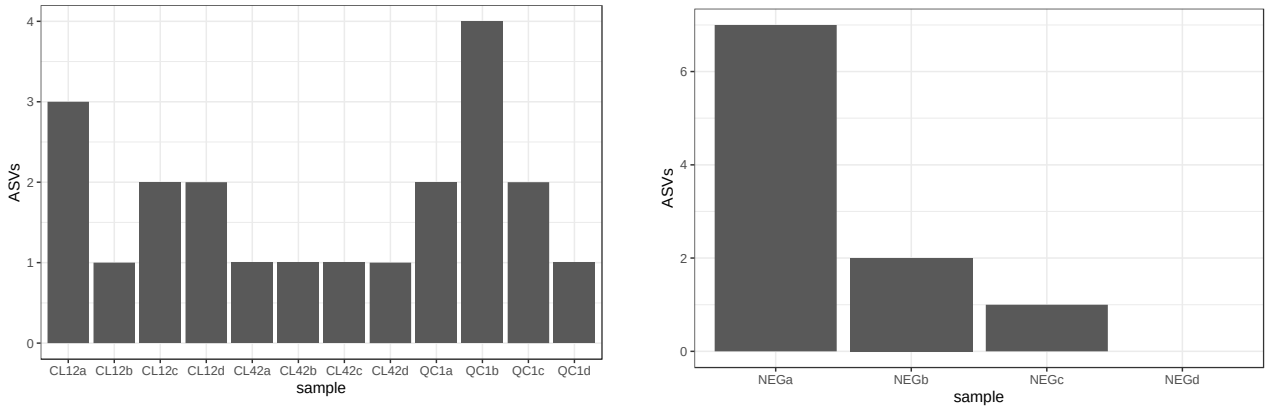

The number of ASVs assigned to both positive (A) and negative (B) controls. The low number of ASVs assigned per positive control suggests high assignment specificity from the DADA2 algorithm and the low number of ASVs assigned to negative controls suggests low rates of sequence jumping.

Figure 10: Mass-length relationships by species graph

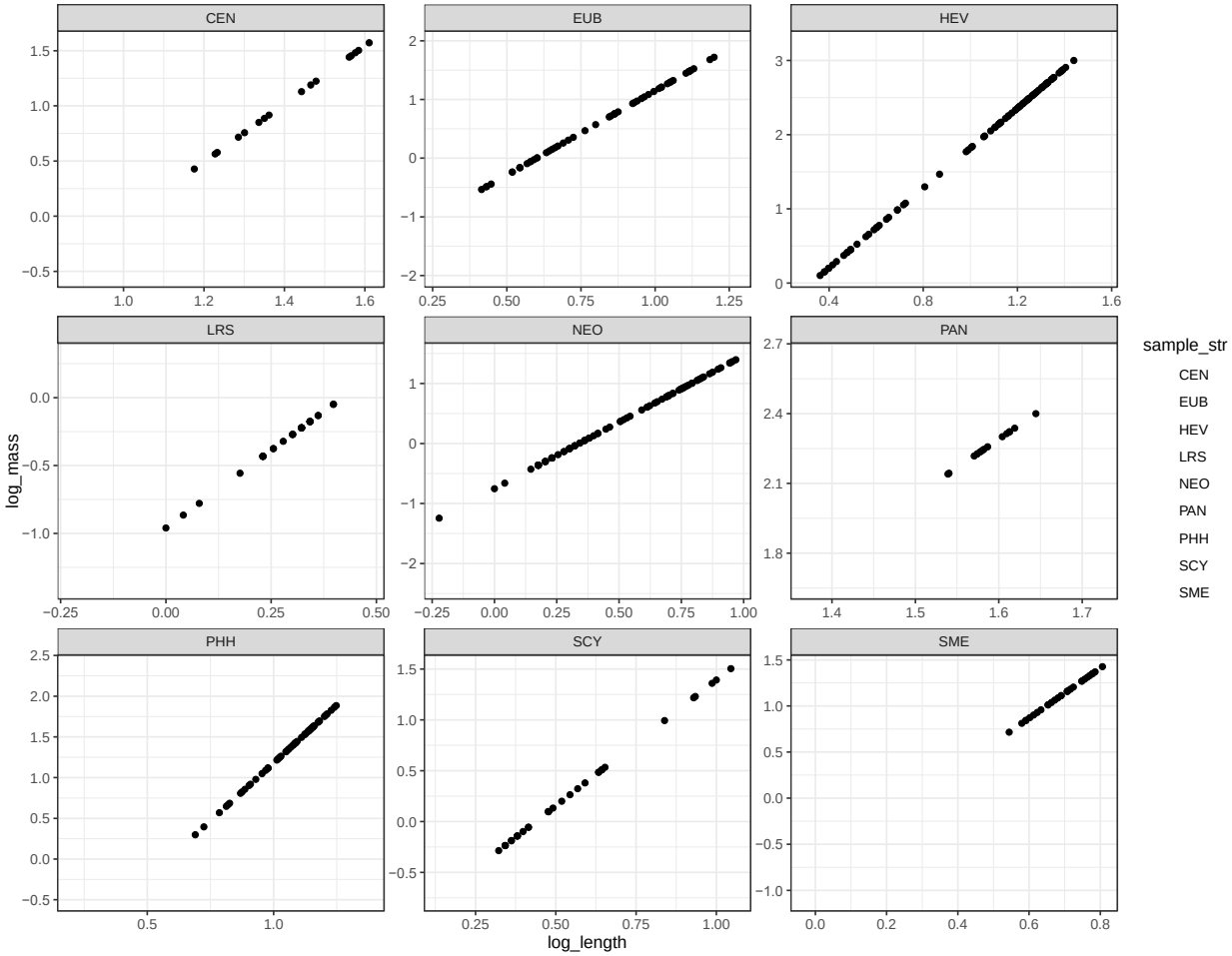

We predicted the mass of predators in this study based on mass-length relationships from predators from Palmyra Atoll and the literature. Plotted are each species' $\log_{10}$-$\log_{10}$ mass-length relationships, with the lines and black dots indicating predicted values for predator individuals in this study and the grey background dots the distributions of those predators used to build those models. We predicted predator mass with a linear mixed effects model of predator mass predicted by predator length with a random slope and intercept of predator species by size, such that the per-species slope could vary. This model had a significant by-species length-mass relationship ($\beta = 2.58$, p-value < 0.001, $R^2_m = 0.69$ and $R^2_c = 0.95$.

Figure 11: Phylogenetic tree of prey items

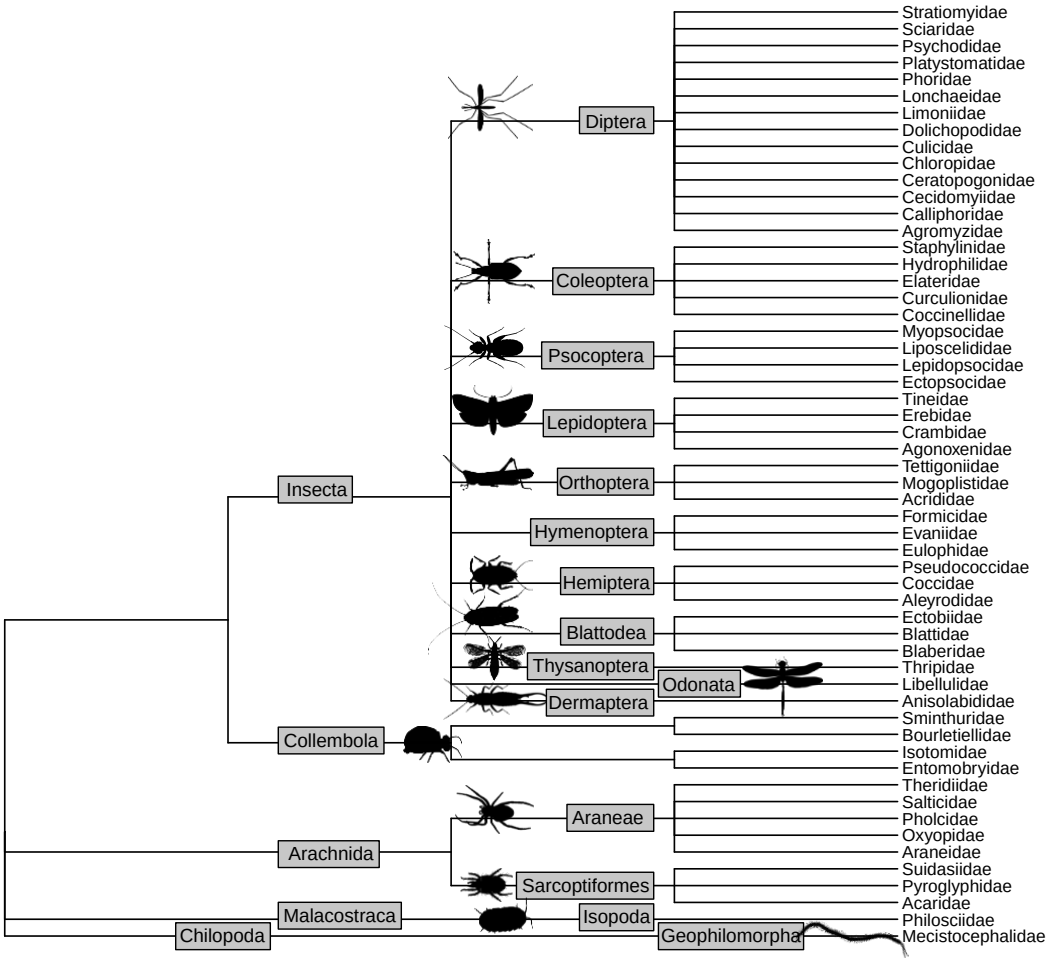

A phylogenetic tree of the prey identities from DNA diet data. Predators consumed 55 families of 16 arthropod orders.

Figure 12: Prey size distribution. Prey family average size spans between $3.8x10^{-4}$ to $3.1x\ 10^{2}$.